수직 연료 분사기구를 포함하는 HyShot 스크램제트 연소기의 동적 연소 유동해석

원수희[*]·정인석[**]·최정열[***][†]

Numerical Analysis of Dynamic Combustion in HyShot Scramjet Combustor with a Transverse Fuel Injection

Su-Hee Won, In-Seuck Jeung and Jeong-Yeol Choi

ABSTRACT

This paper describes numerical efforts to investigate combustion characteristics of HyShot scramjet combustor, where gaseous hydrogen is transversely injected into a supersonic cross flow. The corresponding altitude, angle of attack, and equivalence ratio are 35-23 km, 0°, and 0.426 respectively. Two-dimensional simulation reasonably predicts combustor inner pressure distribution and reveals periodic combustion characteristics of HyShot scramjet combustor. Altitude effects are also investigated and the strength of flow instability and subsonic boundary layer thickness affect the combustion efficiency according to altitudes. Frequency analyses provide the flow instability effects on the turbulent combustion in HyShot scramjet combustor.

Key Words: Scramjet Combustor, Transverse Injection, Flow Instability, Frequency Analyses

1. Introduction

Hypersonic air-breathing propulsion engine is the key issue for the success of future high-speed air transportation. Although there are many technical challenges for the hypersonic engine, combustor is one of the core technologies. The flow entering a combustor at hypersonic flight speed should be maintained supersonic to avoid the excessive heating and dissociation of air. The residence time of the air in a hypersonic engine is on the order of 1 ms for typical flight conditions. The fuel must be injected, mixed with air, and burned completely within such a short time span. A number of studies have been carried out and various concepts have been suggested for scramjet combustor configurations to over come the limitations given by the short flow residence time. Among the various injection schemes, transverse fuel injection into a channel type of combustor appears to be the simplest and has been used in several engine programs, such as HyShot[1] scramjet engine, an international program leaded by the University of Queensland(UQ).

From the aspect of fluid dynamics, transverse injection of fluid into a supersonic cross flow is a significant interest topic due to its broad applications in many engineering devices. Extensive efforts have been applied to study these phenomena, and many of the results have great relevance to scramjet combustors. Papamoschou and Hubbard[2] observed the fluid dynamic instability of

* 학생회원, 서울대학교 대학원 항공우주공학과
† 연락저자, E-mail : aerochoi@puasn.ac.kr
** 정회원, 서울대학교 항공우주공학과
*** 정회원, 부산대학교 항공우주공학과

injection flow. Ben-Yakar et al.[3] also observed essentially the same unstable injection jet in their supersonic combustion experiment. The unsteady nature of transverse injection flow has been first studied numerically by von Lavante et al.[4] but its physical nature has been discussed less importantly. A comprehensive study directly applied to combustor dynamics, however, is rarely found. The obstacles lie in the difficulties in conducting high-fidelity experiments and numerical simulations to characterize the flow transients at time and length scales sufficient to resolve the underlying mechanisms. The present study attempts to achieve improved understanding of unsteady flow and flame dynamics in a real scramjet combustor configuration employing a transverse fuel injection.

2. Numerical Approach

2.1 Governing Equations and Numerical Methods

The flowfield is assumed to be two-dimensional for computational efficiency, and can be described with the conservation equations for a multi-component chemically reactive system. The coupled form of the species conservation, fluid dynamics, and turbulent transport equations can be summarized in a conservative vector form as follows.

$$\frac{\partial Q}{\partial t} + \frac{\partial F}{\partial x} + \frac{\partial G}{\partial y} = \frac{\partial F_v}{\partial x} + \frac{\partial G_v}{\partial y} + W \quad (1)$$

The governing equations were treated numerically using a finite volume approach. The convective fluxes were formulated using Roe's FDS method derived for multi-species reactive flows along with the MUSCL approach utilizing a differentiable limiter function. The spatial discretization strategy satisfies the TVD conditions and features a high-resolution shock capturing capability. The discretized equations were temporally integrated using a second-order accurate fully implicit method. A Newton sub-iteration was also used to preserve the time accuracy and solution stability.

2.2 Chemistry Model and Turbulence Closure

The present analysis employs the GRI-Mech 3.0 chemical kinetics mechanism for hydrogen-air combustion. The mechanism consists of nine species (H, H_2, O, O_2, H_2O, OH, H_2O_2, HO_2 and N_2) and twenty-five reaction steps. Turbulence closure is achieved by means of Mentor's SST (Shear Stress Transport) model. One of important issues is the closure problem for the interaction of turbulence and chemistry in supersonic conditions. Recently, there were many attempts to address this issue using LES methods, PDF approaches, and other combustion models extended from subsonic combustion conditions. Although many useful advances were achieved, the improvement was insignificant in comparison with the results obtained from laminar chemistry and experimental data, as discussed by Möbus et al[5]. A careful review of existing results, such as Norris and Edwards[6] suggests that the solution accuracy seems to be more dependent on grid resolution than the modeling of turbulence-chemistry interaction. In the lack of reliable models for turbulence-chemistry interactions, especially for supersonic flows, the effect of turbulence on chemical reaction rate is ignored in the present work.

3. Scramjet Combustor Configuration

3.1 Combustor Configuration

T4 shock tunnel of UQ was used for the ground test under the conditions M=6.5, p=0.9-5.8 kPa and T=285-291 K. From the given conditions the total enthalpy is 3.0 MJ/kg. The scramjet consists of an intake, a combustor and a thrust plate and each size of components is of 305 mm×100 mm, 300 mm×75 mm and 200 mm×75 mm respectively. The intake is a 17° inclined wedge which compresses the incoming hypersonic flow. The flow is further compressed by the combustor cowl, after which hydrogen is injected. Combustion occurs in the combustor and hot gases from the combustion process are expanded through the thrust plate hence producing thrust. Figure 1 describes the experimental model and computational grid.
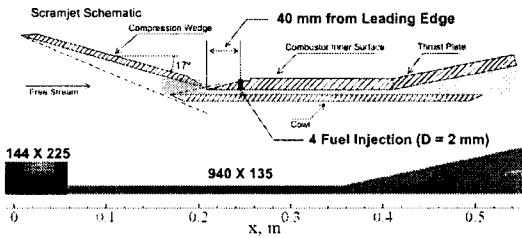
Fig. 1 HyShot model scramjet for ground test and grid system

The combustor has a constant rectangular area and 16 pressure transducers which are mounted orderly 90 mm downstream from the combustor inner surface leading edge. Each distance between pressure transducers is 13 mm. The thrust plate has a 12° inclined plate and 11 pressure transducers which are mounted orderly 11 mm downstream from the combustor exit. The distance between each pressure transducer is also of 13 mm. Four injectors with a 2 mm diameter are located 40 mm downstream from the combustor inner surface leading edge with hydrogen injected transversally into the incoming supersonic flow. For the two-dimensional numerical analysis, the four fuel injectors were assumed to be one long slot of 75 mm × 0.168 mm with the same area.

3.2 Operating Conditions

In the flight test the sounding rocket reaches a maximum altitude of 315 km and the scramjet is maneuvered into the experimental attitude before re-entry. Between altitudes of 35 km and 23 km, gaseous hydrogen is injected into the scramjet and pressure measurements are recorded. During the flight, the scramjet/rocket vehicle exposes changing conditions such as altitude(h), angle of attack(AOA), equivalence ratio(ϕ), spin, etc. Among these variations, the ground experiment using T4 free piston shock tunnel considered altitudes (h=35, 28, and 23 km), angle of attack (AOA=0°, 4°, and −4°) and equivalence ratios (ϕ=0-0.75). The simulation focuses on the design point which corresponds to h=28 km, AOA=0°, ϕ=0.426 respectively. In addition, two more cases (h=35 and 23 km) are simulated to explain the effects according to altitude. The experimental data were taken about 1.2 ms after the flowfield was established in the

combustor and the same procedure was followed in simulations. The detail conditions are summarized in Table 1 for freestream, combustor inlet, and injector exit.

Table 1. Simulation conditions

	Freestream	Combustor Inlet	Fuel Injector
h=35km, AOA=0°, ϕ=0.426			
p [kPa]	0.95	32.74	113.72
T [K]	306	1161	250
M	6.53	2.75	1.0
h=28km, AOA=0°, ϕ=0.426			
p [kPa]	2.22	82.11	307.34
T [K]	311	1229	250
M	6.75	2.79	1.0
h=23km, AOA=0°, ϕ=0.426			
p [kPa]	5.47	188.05	648.60
T [K]	307	1164	250
M	6.53	2.75	1.0

4. Results and Discussion

4.1 Grid Refinement Study

A matrix of 12 cases was considered that covers possible combinations of y+ and grid resolution. In order to examine effects of grid resolution on the discretization error, three levels of combustor girds consisting of Level 1 (625×90), Level 2 (940×135), and Level 3 (1,435×202) were generated. The refinement factor between coarse and fine grid was maintained 1.5 and each level had four different wall-clustering factors to examine effects of y+ sensitivity on the turbulence model. Figure 2 as a part of grid refinement results describes Mach contour around fuel injector according to grid resolution. The Mach contour was basically taken under the same condition and physical time except grid system. Overall combustor flowfields are similar each other but the detail flow structures are different, especially in Level 1 grid. In the case of Level 1, the size and shape of a downstream recirculation region are much different from the other two cases. The large separation bubble on the upper combustor wall is also invisible in Level 1, even though it is clearly seen in Level 2 and Level 3 grid at the same position. Finally, the boundary layer on the bottom combustor wall
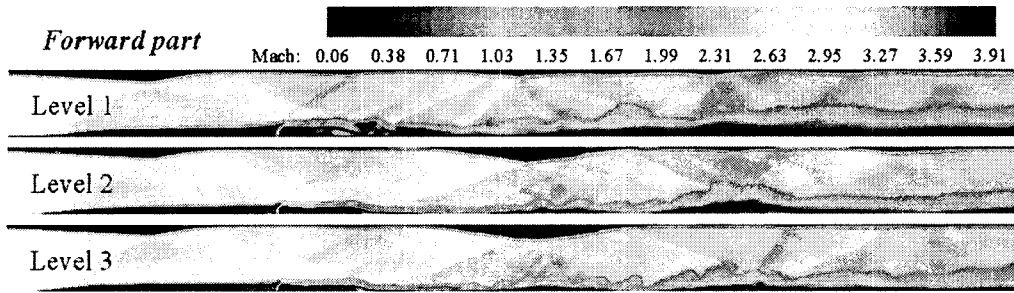
Fig. 2 Mach contour around fuel injector according to grid resolution

of Level 1 is thicker than the other two cases. The above observations show that the Level 1 grid does not show spatial and temporal convergence. Therefore, the higher resolution grid like Level 2 or Level 3 is needed for this simulation and Level 2 is more proper for both numerical convergence and computational efficiency.

For the quantitative assessment of grid quality, the upstream separation distance (x_{sep}) and combustion efficiency (η_C) were compared at design condition. The separation distance is measured from the turning point of velocity value at wall and the combustion efficiency is defined as

$$\eta_C(x) = 1 - \frac{\int \rho u y_F \, dA}{\left(\int \rho u y_F \, dA\right)_{x=0}} = 1 - \frac{\dot{m}_F}{(\dot{m}_F)_{x=0}} \quad (2)$$

As the grid level increases, separation distance increases from 33.4 to 34.7 mm and combustion efficiency increases from 55.5 % to 62.7 %. Grid convergence index(GCI)[7], a methodology for the uniform reporting of grid refinement study, was calculated to estimate the quantitative discretization error in a given gird systems and the numerical uncertainty was suppressed within 3 %. Table 2 illustrates this calculation procedure and detail values. Thus, the turbulent combustion flow in HyShot combustor was simulated in Level 2 grid where y+ was below 1.

Table 2. GCI by x_{sep} and η_C

	x_{sep}	η_C
Level 1	33.4 mm	55.5 %
Level 2	34.3 mm	61.8 %
Level 3	34.7 mm	62.7 %
GCI$_{23}$	2.7 %	2.4 %

4.2 Surface Pressure and Flow Instability

Numerical simulations for the design conditions listed in Table 1 were performed to simulate the pressure distribution of HyShot scramjet combustor. As mentioned in Sec 3, pressure measurements were recorded using 16 pressure transducers mounted along the centerline of combustor inner surface. The first one is located 50 mm downstream from the fuel injector and each interval is 13 mm. The experimental pressure distributions were extracted at 1.2 ms after the flowfield was established in the combustor and the same procedures were repeated in the unsteady simulations.

Numerically obtained surface static pressure distributions and experimental data for design condition are compared with each other in Fig. 3. The pressure rise due to combustion is observed from experimental data, particularly towards the rear of the combustion chamber. The pressure rising tendency is also observed in the computational results but the rising slope is gentle compared with experiment. The simulation slightly overpredicts surface static pressure at the forward part of the combustor and the opposite situation occurs at the backward part of the combustor. Much of the difference between experimental and numerical results seems to be attributed to the absence of three-dimensional flow structures. However, the surface static pressure distributions reasonably agree with each other for the most part.

The temporal variations of a combustor surface pressure are shown in Fig. 4. The pressure is recorded at 5, 14, and 23 cm from the fuel injector and these measurement points correspond to #1, #8, and #15 pressure
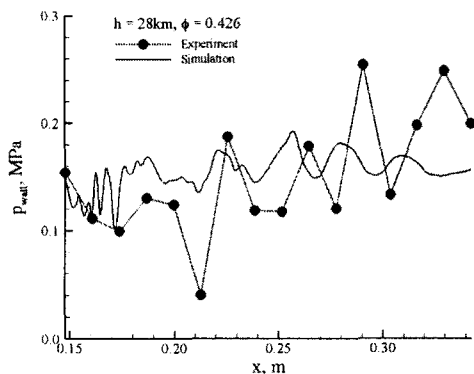
Fig. 3 Surface pressure profile between experiment and simulation
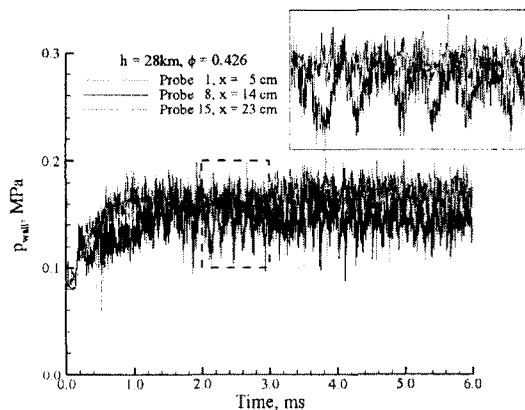

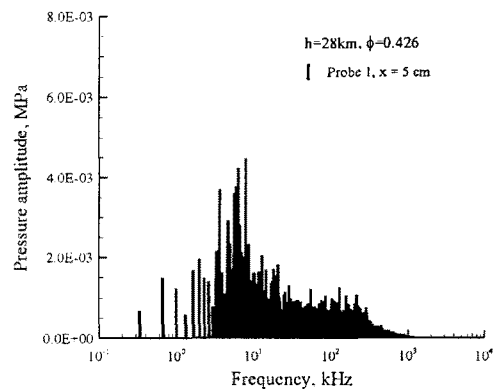Fig. 4 Pressure-time history at x=5, 14, 23 cm from fuel injector

Fig. 5 Frequency spectrum of pressure at x=5 cm from fuel injector

transducers respectively. For all measurement points, oscillating pressure characteristics are observed except for an initial pressure buildup region until about 1 ms. The mixed states between high-frequency and low-frequency appear in the graph and this phenomena show the unsteadiness of turbulent combustion in HyShot scramjet combustor. The pressure-time history of #1 transducer reveals clear periodic characteristics as well (see insert of Fig. 4). For a detail analysis of periodic characteristics, the frequency spectrum of #1 transducer data was obtained using FFT (Fast Fourier Transform) and was displayed in Fig. 5. Only 1 to 6 ms time period was considered in FFT analysis to exclude the transient effects at initial phase. Although it is not easy to identify a clear principal frequency due to the frequency mixed-up and transient nature of a pressure-time history, the frequency spectrum shows that principal frequency is about 8 kHz.
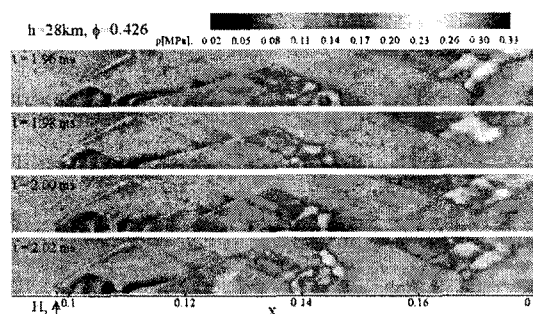

Fig. 6 Temporal variation of pressure flowfield

Pressure contours with time are revealed in Fig. 6 to investigate the periodic oscillating pressure effects on the combustor flowfield. The figures which include flow structures around injector are displayed from 1.96 to 2.02 ms at an interval of 0.02 ms. The Richtmyer-Meshkov instability is triggered by the interaction between the impinging oblique shock wave and fuel-air shear layer. The generated instability is propagated into upstream through the subsonic boundary layer and disturbs the downstream recirculation region. It, however, does not trigger the injection flow to become unstable and then flows to downstream. The turbulent mixing and combustion are enhanced as a result of the increase of a fuel-air interface as shown in figures. These processes are repeated and recorded in the pressure-time history.
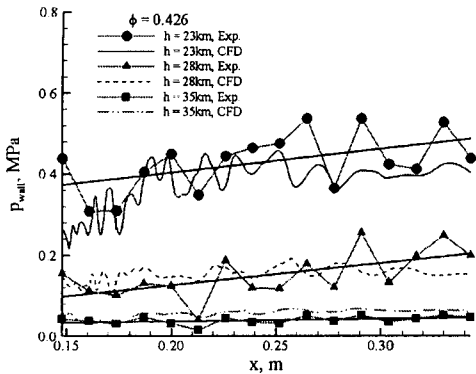
4.3 Altitude Effects

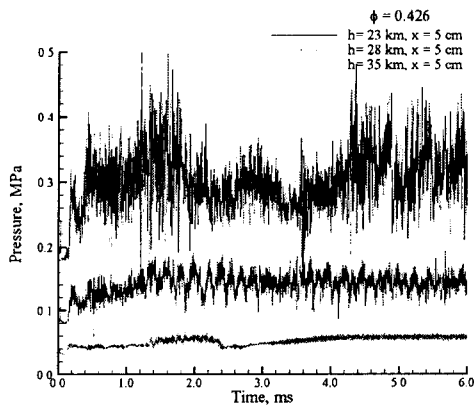Fig. 7 Surface pressure profile between experiment and simulation along altitude

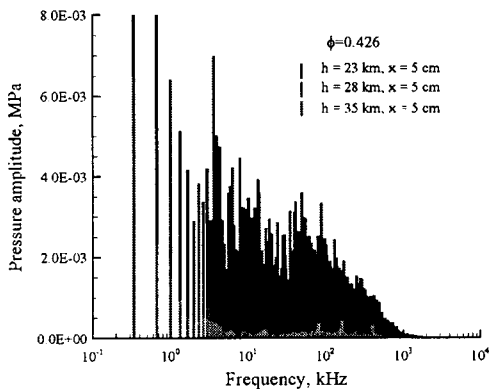Fig. 8 Pressure-time history at x=5 cm from fuel injector along altitude

Fig. 9 Frequency spectrum of pressure at x=5 cm from fuel injector along altitude

Numerical simulations for the off-design conditions listed in Table 1 were performed to examine altitude effects on HyShot scramjet combustor. As an altitude decreases from 35 to 23 km, only the pressure varies significantly and the other mean flow conditions are maintained in design conditions.

The surface static pressure distributions between numerical and experimental data along altitude are compared each other in Fig. 7. The pressure rising tendency are common regardless of altitude as the measurement point moves towards the rear combustor, but the pressure rising slope increases with an altitude decrease in both experimental and simulation results. The pressure distributions from two-dimensional simulations reasonably agree with all experimental cases.

The temporal variations of a combustor surface pressure along altitude are shown in Fig. 8. As the previous paragraph, the pressure is recorded at 5 cm from the fuel injector and this measurement point corresponds to #1 pressure transducer. The pressure-time history of altitude of 28 km shows periodic characteristics, but the other two altitude cases show very irregular behaviors. The flowfield becomes considerably unstable with high amplitude and long wavelength for altitude of 23 km and approaches relatively stable in about 3 ms for altitude of 35 km. For a more quantitative analysis of the oscillating pressure -time history along altitude, the frequency spectrum of pressure transducer data was compared using FFT in Fig. 9. The data sampling range corresponds to the previous case which ranges from 1 to 6 ms. The dominant frequencies, altitude of 23 and 28 km, are about 4 and 8 kHz respectively. In the case of altitude of 35 km, the pressure-time history is dominated by high frequency and a specific dominant frequency is not observed. The principal frequency, therefore, tends to move toward low frequency as altitude decreases.

Figure 10 shows the density contours and distinct differences are observed. According to an altitude decrease, the subsonic boundary layer thickness as well as the strength of Richtmyer-Meshkov instability increases. Here the subsonic boundary layer is a passage which the instability propagates through. As a
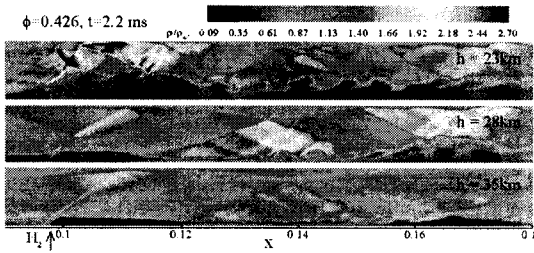
Fig. 10 Density contour comparison along altitude

result of above effects, there exist an ordinary instability in 23 km altitude, a periodic instability in 28 km altitude, and a flow converging to stable state as an initial instability disappears in 35 km altitude. The combustion efficiencies along the altitude increase are 83.5, 61.8, and 45.0 % respectively and therefore the pressure rising slope increases with an altitude decrease. From the above frequency analyses and combustion efficiencies, the unsteadiness of turbulent combustion in the present study is related with intrinsic supersonic flow instability including a high frequency as well as thermo-fluidic instability including a low frequency.

5. Summary and Conclusion

The turbulent combustion flow in HyShot scramjet combustor was carefully studied by means of a comprehensive numerical analysis. The simulations focused on the design condition (h=28 km, AOA=0°, ϕ=0.426) and were extended to off-design conditions to investigate altitude effects. For the systematic approach, grid refinement study was performed using grid convergence index and discretization error was suppressed within 3 % error band.

Comparisons between experimental and numerical results present that the two-dimensional simulations reasonably predict pressure distributions in combustor. The temporal variations of a combustor wall pressure and frequency analyses using FFT reveal periodic characteristics and the principal frequency is about 8 kHz. These periodic characteristics can be explained by the Richtmyer-Meshkov instability propagation. Altitude effects are also investigated as off-

design conditions. The residence time of instability is controlled by the strength of instability and subsonic boundary layer thickness. This affects the combustion efficiency and pressure rising slope according to altitudes. Finally, the unsteadiness of turbulent combustion related with intrinsic supersonic flow instability including a high frequency as well as thermo-fluidic instability including a low frequency.

후 기

참고문헌

[1] Centre for Hypersonics - HyShot Scramjet Test Programme, http://www.mech.uq.edu.au/hyper/hyshot/

[2] Papamoschou, D., and Hubbard, D.G., "Visual Observations of Supersonic Transverse Jets," *Experiments in Fluids*, Vol. 14, May 1993, pp. 468-471.

[3] Ben-Yakar, A., Kamel, M .R., Morris, C. I. and Hanson, R. K., "Experimental Investigation of H_2 Transverse Jet Combustion in Hypervelocity Flows," AIAA Paper 1997-3019, 1997.

[4] Von Lavante, E., Zeitz, D. And Kallenberg, M., "Numerical Simulation of Supersonic Airflow with Transverse Hydrogen Injection," *Journal of Propulsion and Power*, Vol.17 No.6, 2001, pp.1319-1326.

[5] Möbus, M., Gerlinger, P. and Brüggermann, "Scalar and Joint scalar-Velocity-Frequency Monte Carlo PDF simulation of Supersonic Combustion," *Combustion and Flame*, Vol. 132, 2003, pp.3-24.

[6] Norris, J. W. and Edwards, J. R., "Large-Eddy Simulation of High-Speed Turbulent Diffusion Flames with Detailed Chemistry," AIAA Paper 1997-0370, 1997.

[7] Won, S., Jeung, I., Choi, J., "DES Study of Transverse Jet in a Supersonic Crossflows," AIAA Paper 2006-1227, 2006.